Chapter 11

Use of Silver Nanoparticles as Toughening of Alumina Ceramics

Enrique Rocha-Rangel, Azucena Pérez-de la Fuente,
José A. Rodríguez-García,
Eddie N. Armendáriz-Mireles and
Carlos A. Calles-Arriaga

Additional information is available at the end of the chapter

http://dx.doi.org/10.5772/intechopen.76949

Abstract

In this work, alumina/silver composites were produced through powder techniques, which involve the combination of high energy mechanical milling combined with sintering in the presence of a liquid phase and with the idea of having ceramics with good toughness values. From mechanical characterizations, it was found that increases of the silver content in the alumina origins decrease the elastic's modulus and flexural strength of the final composite. The fracture toughness of alumina increases from 4.2 $MPam^{-0.5}$ for monolithic alumina to 10 $MPam^{-0.5}$ for alumina with 2 wt% silver additions. It was determined that the reinforcement mechanism of these materials is due to the deflection of cracks owing to metallic bridges formed by the silver used as toughener material.

Keywords: silver reinforcements, fracture toughness, alumina, silver nanoparticles, ceramic composites

1. Introduction

Manufacturing, in its broadest sense, is the process of converting raw material into a finished product. It includes the design of the product, the selection of the raw material and the sequence of processes and operations through which it will be manufactured [1]. This method exists since approximately 5000–4000BC. The manufacture of products for various uses began with the production of articles made of wood, ceramics, stone, and metal. The materials and

processes that were first used to form products through smelting and forging have been developed gradually over the centuries, using in the actuality new materials and more complex operations, at increasing production rates and higher levels of quality [1].

In the modern sense, manufacturing involves the manufacture of products from raw materials through various processes, machinery, and operations, through a well-organized plan for each required activity [1]. Each approach is suitable only for producing just a particular component and material, and it cannot be used to do all types of products. In reality, the sequence of the manufacturing process is designed according to the requirements of the component to be manufactured.

The metallurgy of powders has been used since 300 BC when massively large iron objects were manufactured [2]. In 1829, new developments were achieved in this area when an English engineer applied cold pressure and sintered platinum powder to produce ductile platinum. Later, in 1870, osmium filaments were made using the powder metallurgy method. In 1916 a commercial tungsten cable manufactured employing this method was also produced. After all these developments in the field of powder metallurgy, a wide variety of components are currently manufactured, such as tungsten carbide cutting tools, refractory parts, and electronic components, among many others [2].

Until now the techniques of processing of powders involve working with very fine powders with sizes of the order of microns, where materials with excellent physical and chemical properties have been obtained. However, with the advance of science, researchers have observed that it is possible to get materials with much better properties working with powders finer than microns. These studies at nanometric levels are what have given way to the nanotechnology and the development of the nanostructured materials. Nanotechnology is a current issue that involves several branches of science, so it is difficult to define it. However, it could be said that it is the design, manufacture, and application of nanostructures or nanomaterials, and the knowledge of the relationships between physical properties or phenomena and the dimensions of the material [3].

The search for new nanostructured functional materials has focused on nanometric scale manipulation, which leads to the improvement of properties at the macro scale [4].

Nanomaterials are a new class of materials (whether they are ceramic, metals, semiconductors, polymers, or a combination of these) in which at least one of their dimensions is between 1 and 100 nm; represent a transition between molecules and atoms and a material with solid volumetric dimensions [5, 6].

At the end of the previous century, there is a classification of these advanced materials called functional materials with a gradient [7]. The functional materials with gradient represent those advanced materials that comprise a particular gradient in structure composition, or both, and adapted for a specific application or function [8]. Ceramic materials in recent years have been developed as advanced materials, and above all, as functional materials with a gradient, due to the favorable properties that they possess and the many ways in which they can be processed [9–14]. They are compounds formed by metallic and non-metallic elements; with general properties that characterize them, it can be pointed out that they are hard, fragile, and resistant to compression; some are transparent, others translucent. Regarding the conductivity

of heat and electricity, some are insulators, others have low conductivity, although this is subject to several factors; they are mostly resistant to corrosion at room temperature and others also at high temperatures [15].

However, the ceramic materials in general present great fragility, in the particular case of the materials made of alumina (Al_2O_3) are not the exception. Alumina is a very useful and widely used industrial ceramic material. Its applications include cutting tools, dental implants, prostheses, electrical and thermal insulations, and wear resistant. Its utility is attributed to its high hardness, high resistance to compression, and high properties of electrical and thermal insulation. However, despite its desirable and potential characteristics, its use as a structural material has been considerably hindered due to its low resistance to fracture (as is typical of ceramics) [9]. Ceramic materials can be made more robust by incorporating fine metal particles into their matrix. This development has been successfully used before in different systems [9, 16–19].

Researchers have used numerous methods aimed at improving fracture toughness and other mechanical properties of alumina processing. In these studies, different systems have been prepared with an alumina-based ceramic matrix reinforced with the incorporation of metallic particles presenting the following results: Yao [20] has applied spark plasma sintering for the preparation of Al_2O_3/Ni nanocomposite and has reported a fracture toughness of 3.84 $MPam^{-0.5}$. Sekino [21] has prepared an Al_2O_3/Ni nanocomposite by hot pressing of an Al_2O_3/NiO mixture at a pressure of 30 MPa and temperature of 1450°C, reporting a resistance of more than 1 GPa, but the fracture toughness was only 3.5 $MPam^{-0.5}$ for 5% by volume of Ni content. So from this investigation, it was concluded that the Ni increases only nominally the fracture toughness, even though the nickel is appreciably ductile. The lack of coincidence of the coefficient of thermal expansion between nickel and alumina could be responsible for the reduction of gain in fracture toughness. Guichard [22] has reported the production of Al_2O_3/Cr composites with fracture toughness values between 4 and 7.2 $MPam^{-0.5}$ by varying only the chromium content. The densification of these composites was carried out by sintering without pressure, and hot pressing at temperatures between 1400 and 1600°C. The samples of the hot pressing proposed work were much denser and with higher hardness than those sintered without pressure. Ji and Yeomans [23] have manufactured an Al_2O_3/Cr nanocomposite containing 5% by volume of chromium, registering a strength and fracture toughness of 736 MPa and 4.72$MPam^{-0.5}$, respectively. Therefore, they concluded from this study that a relatively high chromium content is necessary for the improvement of fracture toughness. In his research, Prielipp [24] has used Al_2O_3/Al and the gas pressure infiltration for the porous alumina reinforcement. He has obtained a resistance of 810 MPa and a fracture toughness of 10.5 $MPam^{-0.5}$, this result was registered in a composite with 35% aluminum volume. These values are remarkable in comparison with the values corresponding to the non-reinforced monolithic alumina. Another notable feature of this compound is that both fracture strength and fracture toughness were significantly improved without compensation. Although 35% by volume of aluminum was concluded in this work, it is a significantly high amount for reinforcement, since the fact that aluminum is of a density much lower than alumina making this percentage of values comfortable [25]. In different studies, authors comment that the reinforcement models indicate that the size of the metal inclusion and the homogeneous distribution of it in the ceramic matrix are critical to ensure obtaining a composite material with favorable tenacity properties [9].

In general, to get the best microstructures and properties, a ceramic based compound must be carefully prepared since the powder synthesis stage. Ceramic/metal composite materials have typically been prepared by hot pressing powder mixtures prepared by chemical routes [26–30]. However, there have been problems in the reproduction of their very peculiar properties and their routine use in practical applications of this type of compounds, due to the contamination of the powders during the milling operation, the complexity of the chemical solutions and the costs of producing large quantities of materials by hot pressing. From the review made so far, the Al_2O_3 ceramics have not been reinforced with silver, despite the excellent ductility of silver, in such a way that it would be very interesting to determine the effect of silver on fracture toughness of Al_2O_3-based ceramics. In this way the objective of this study is; to fabricate alumina-based ceramic materials (Al_2O_3) reinforced with Ag (silver) nanoparticles through mechanical grinding and pressureless sintering and to determine the effect of silver on the fracture toughness of alumina.

2. Experimental

This chapter describes the experimentation carried out detailing each of the working conditions in each stage of the process, for obtaining the alumina-based composites with silver nanoparticles and the characterizations made in the obtained materials to determine their mechanical properties, mainly fracture toughness.

2.1. Powders

The starting materials were alumina (Al_2O_3) powder (Sigma-Aldrich, 5 μm size and 99.9% purity), silver (Ag) powder (Mayer, 1 μm size and 99.9% purity).

2.2. Milling

The final contents of silver in the alumina-silver composites were: 0.0, 0.5, 1, 2, and 3% weight. The grinding and mixing of the powders were carried out in a planetary type mill (Retsch, PM100 German), in dry for 3 h with turning intervals every 3 min, at a rotation speed of 250 rpm. It was used a 250 ml stainless steel container with ZrO_2 zirconia grinding elements (0.3 cm diameter), the ratio between the weight of the balls and the powder weight was 12:1.

2.3. Powder granulometry

After the grinding stage for each of the samples, a granulometric analysis of the powder was carried out (Malvern Instruments, Masterziser 2000, England); this equipment uses the laser diffraction technique to measure the size of the particles suspended in an aqueous solution.

2.4. Compaction

With the powders obtained from the milling, and with the help of a steel die tool grade they were manufactured cylindrical samples. The dimensions were of 2 cm diameter by 0.3 cm thickness with an approximate weight of 2 grams; the compaction of said samples was carried out at room temperature, by uniaxial pressing using 350 MPa in a hydraulic press (Montequipo, LAB-30-T, Mexico).

2.5. Density of samples in green

The measurements of the densities of green samples (before sintering) were obtained through direct measurements taking the diameter and the thickness in millimeters with a digital calibrator (Mitutoyo, D6CS, Japan) to register their volume. The weight in grams was obtained through a digital balance (A&D, HR-120, Japan). Once these measurements were made, the real green density was calculated using a ratio of mass to volume, taking the following formulas:

$$V_s = \pi r^2 h \tag{1}$$

$$\rho_r = \frac{W_s}{V_s} \tag{2}$$

where V_s is the sample's volume (cm^3), r is the sample's radius (cm), h is sample's height (cm), ρ_r is the sample's real density (gcm^{-3}), and W_s is the sample's weight (g). In the same way, theoretical density of each composition was calculated by the rule of mixtures according to the following formula:

$$\rho_t = (\rho_t Al_2O_3)(X\,Al_2O_3) + (\rho_t Ag)(X\,Ag) \tag{3}$$

where $\rho_t Al_2O_3$ is the theoretical density of alumina (3.98 gcm^{-3}), $\rho_t Ag$ is the theoretical density of silver (10.5 gcm^{-3}), $X\,Al_2O_3$ is the molar fraction of alumina and $X\,Ag$ is the molar fraction of silver. Finally, we proceed to calculate the relative density of each sample with the following formula:

$$\rho_{rel} = \frac{\rho_r}{\rho_t} \times 100 \tag{4}$$

2.6. Sintering

The pressed samples were subjected to different sintering cycles, using temperatures of 1400, 1500, and 1600°C, during sintering times of 1, 2, and 3 h. For this, an electric furnace was used (Carbolite, RHF17/3E, England) with super Kanthal resistances, a heating rate of 5°Cmin^{-1} was used in all cycles, in each sintering cycle, an argon gas flow of 10 cm^3 min^{-1} was injected into the furnace chamber to inhibit the oxidation of silver. The cooling of the pellets was carried out inside the furnace by turning off this once the sintering cycle was completed. The choice of sintering conditions is due to the fact that at temperatures below 1400°C the alumina is not sintered. While, at temperatures above 1600°C, besides there would be an excessive growth of grain, there is a risk that the silver evaporates. Conducting studies at intermediate temperatures between 1400 and 1600°C would not seem to give a different behavior. Something similar happens with the sintering times; at low times there would not be an adequate sintering of the alumina, while longer times would cause grain growth, deteriorating with these the mechanical properties of the final material.

2.7. Density of sintered samples

Once the samples were sintered, the density of each of them was measured using the Archimedes method by placing water in a plastic container, which was placed on a balance and the weight of samples was recorded. Immediately, the temperature of the water was measured with a thermocouple (National Instruments, NI USB-TC01, USA), the time the sample

was submerged in the water was 10 min, this in order that the water was introduced into the porosity and removed the air contained in the sample. Following this procedure and with the water weight readings recorded, the real density of the sintered samples was calculated using the following formula:

$$\rho_r = \frac{(W_s H_2 O)(\rho_{H_2O})}{W_s} \times 100 \quad (5)$$

where $W_s H_2 O$ is the sample's weight in H_2O (g), and ρ_{H2O} is the density of water at the experimental temperature (gcm^{-3}).

2.8. Contraction percentage

Before and after sintering the samples, their diameter was measured with the help of a digital calibrator (Mitutoyo, CD6CS, Japan). With this data, the contraction percentage of each sample was calculated applying the following formula:

$$C_s = 1 - \frac{D_s}{D_v} \times 100 \quad (6)$$

where C_s is the sample's contraction (%), D_s is the diameter of sample heat treated (cm), and D_v is the diameter of sample in green (cm).

2.9. Microstructure

2.9.1. Optical microscopy (OM)

Microstructure observations of each sample were made by optical microscopy, using an optical microscope (Nikon Eclipse, Ma200, Japan). The images were taken at different magnifications and using different light filters, in different parts to observe better details of the microstructure, such as grain growth, the homogeneity of the distribution of silver, and the shape and size of the grain.

2.9.2. Scanning electron microscopy (SEM)

Microstructure observations of each sample were also made by scanning electron microscopy, which allows obtaining better details of the microstructure. Before being analyzed the samples were coated with a layer of graphite to make them conductive, to carry out the observations, 15Kv of acceleration voltage was used in an electron microscope (JEOL, JSM 6300, Japan).

2.9.3. Analysis by energy dispersive of X-rays (EDX)

For this study, it was used a Hitachi equipment (SU9000 UHR FE-SEM, Japan) and the Image plus S-75 software. With which punctual analyzes were made in different areas of the samples, to verify the existing chemical elements in each phase present in the microstructure.

2.10. X-ray diffraction (XRD)

This study was carried out with the help of a Siemens diffractometer (D-5000, German), here it was corroborated the existence of the crystalline phases in the composites.

2.11. Mechanical properties

2.11.1. Elastic modulus

The sintered samples were cut to a rectangular shape and placed on a pair of polyester supports (to avoid absorption of vibration). Then they are hit with a metal hammer, this activity emits a sound which travels through the sample at a certain speed, and this resonance is captured using an ultrasonic sensor (GrindoSonic, A-360, Japan). Subsequently, the equipment has software to which data such as the size of the sample and its density are entered, which calculates the elastic module according to the following expression:

$$E = \rho_r v^{0.5} \tag{7}$$

where E is the sample's elastic modulus (GPa), and v is the sound velocity in the sample (cms^{-1}).

2.11.2. Flexural strength

To measure the flexural strength, it was necessary to cut the samples in a rectangular shape using a diamond disc cutter. For the test, the sample was placed on a pair of supports located at a distance from each other and applying the load just in the center of the sample. During the test, no preload was applied, after this, a head moved at a speed of 0.05 $mmmin^{-1}$ with a cell with a load of 10 GPa to perform the test, the machine that was used to measure the resistance to bending is from the Instron brand with a mobile head.

2.11.3. Microhardness

For the microhardness test, 20 measurements were made in different places of the sample; this was done with a micro durometer (Wilson Instruments, S400, Japan). In each test a force of 9.8 N was applied during 10s, once the indentation was finished, it was preceded to determine the measure of the diagonals d_1 and d_2 of the print (**Figure 1**) and depending on the results and dimensions of this print it can be determined the hardness of the material.

2.11.4. Fracture toughness

To measure the fracture toughness, the same 12 tests of the measurement of microhardness are used, with the measurements of the cracks generated in the vertices of the indentation print and with the dimensions of diagonal of the print; the fracture toughness can be evaluated in agreement with the next equation [31]:

$$K_{1c} = \frac{0.16}{(c/a)^{1.5}} \times (H a^{0.5}) \tag{8}$$

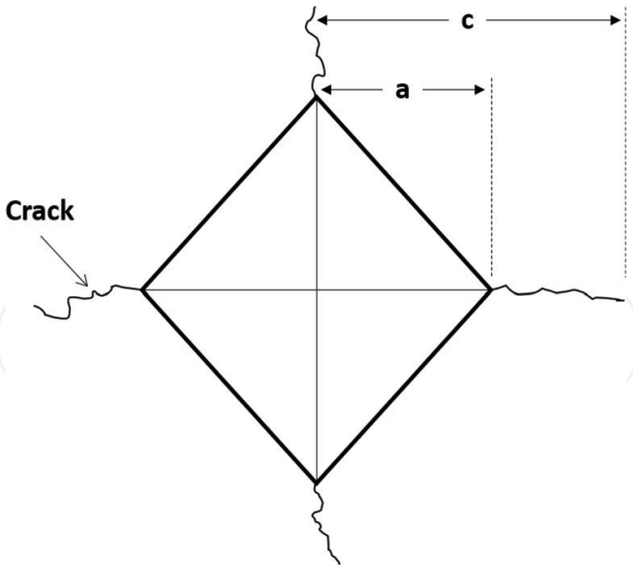

Figure 1. Image showing the cracks generated in the vertices of the indentation print.

where K_{IC} is the critical stress intensity factor in load mode I, H is the Vickers hardness (GPa), c is the average length of the cracks obtained from the tips of the Vickers (μm), and a is the average length of the half of the diagonal of the Vickers (μm).

3. Results

3.1. Morphology and powder size

Figure 2 shows micrographs of mixtures of alumina powders with different percentages of silver. In this figure, there can be visualized very fine particles with nanometric sizes. There can be observed few spherical particles. However, the particles are mostly irregular and dendritic, in the same way in the majority of the samples particle; they have formed agglomerates with sizes greater than 2 microns. Having this homogeneity in the sizes and shapes of the powders will undoubtedly benefit the compaction of the samples and the resulting densification of the same. The observation of the silver particles is difficult due to their nanometric size; however, in the pictures, they observe very small white dots at intergranular positions, and these small dots correspond to silver.

In the graphs of **Figure 3** are shown the results obtained from the granulometric analysis. Based on them, it can be determined that approximately 45% of the powder has particle sizes between 0.1 and 1 microns (nanometer size), about 30% of the powder presents particles between 1 and 10 microns, and about 25% of the particles powders have sizes greater than 10 microns. In some cases, particle sizes are close to 100 microns, and due to the presence in the mixtures of very fine powders with nanometric sizes, surely these large particles are the result of the agglomeration of small powders. In any case, a proper distribution of particle sizes is present in the powder mixtures, with nanometric powders, which must mean large surface areas and therefore many contact points that will favor atomic diffusion during the sintering stage.

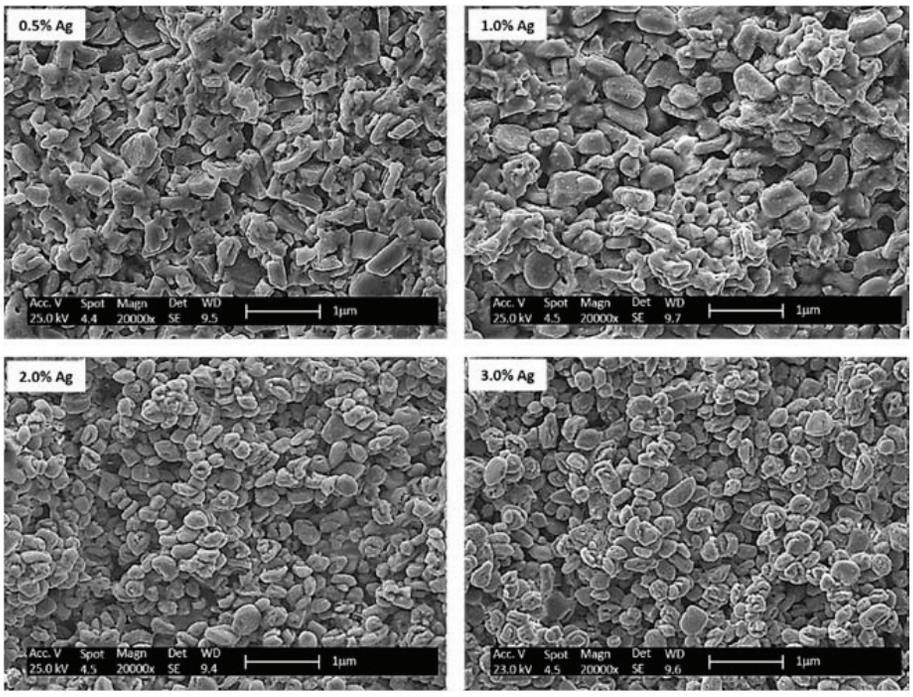

Figure 2. Micrographs of alumina powders with different silver percentages.

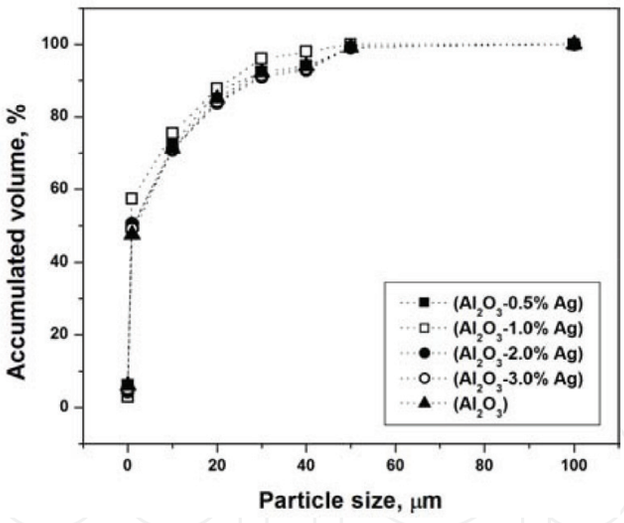

Figure 3. Graphs showing the granulometry of alumina powders reinforced with silver nanoparticles.

3.2. Density

In **Figure 4** are presented the comparison of the results obtained from the densities in green and the densities of the sintered samples for each studied composition. In this figure, it is observed that the density of the sintered samples compared with the samples in green increased considerably. This increase occurred because during the sintering stage the porosity in the samples was reduced due to the homogeneity, shape, and size of the particles. Final density reached by the samples are close to 100%, this means thoroughly densified bodies were obtained after sintering.

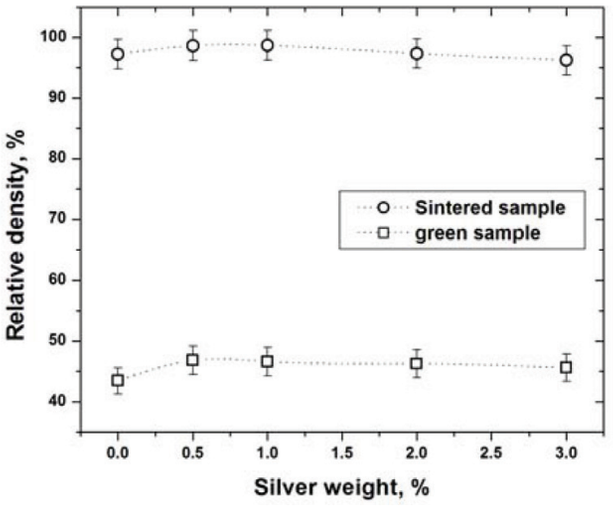

Figure 4. Comparison between green density and sintered density, as a function of silver content in the composite.

3.3. Contraction percentage

In the graph of **Figure 5**, it can be observed the contraction percentages obtained in the samples sintered at 1500°C for 2 h, where the results of previous discussions are reinforced, the samples with inclusions of 0.5–1.0 wt% of Ag obtained a higher percentage of contraction. This means that the more the sample is contracted, the volume decreases due to the elimination of porosity and its density increases. The sample with 0.0% of Ag presents a minimum contraction percentage, well below the other samples, with respect to the samples with inclusions of 2.0–3.0% of Ag; the tendency to decrease with the higher amount of Ag is presented again in these results. Therefore, in agreement with the results, it has that silver present in the composite favor contraction, and therefore, densification of composites. In other words, composites with low porosity were manufactured, which means that there are fewer sites for the initiation and propagation of cracks.

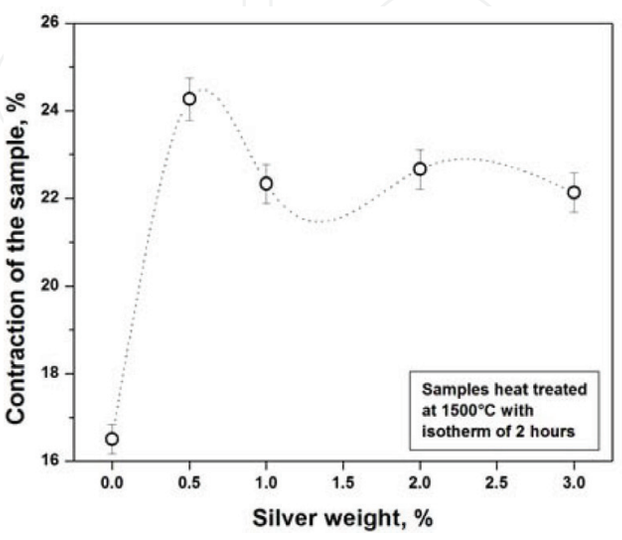

Figure 5. Contraction percentage of the sintered samples at 1500°C, during 2 h.

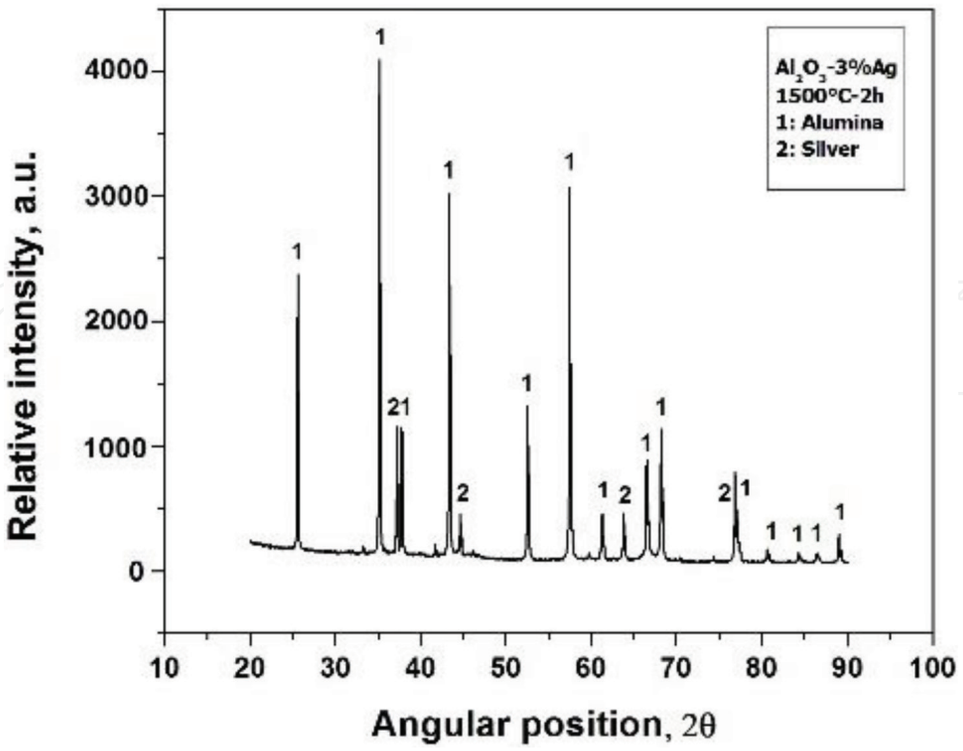

Figure 6. XRD pattern of composite with 3 wt% silver, sintered at 1500°C during 2 h.

3.4. X-ray diffraction of sintered samples

Figure 6 shows the results of the diffraction of x-rays made to the reinforced sample with 3.0 wt% silver. In this figure it can be observed the existence of two phases: The number 1 indicates the presence of alumina and the number 2 indicates the presence of silver, thus obtaining samples without the presence of any possible silver oxide, and this thanks to the argon gas used to protect the atmosphere of the furnace.

By means of the diffraction spectra of **Figure 6**, the particle size for the sample was calculated using the Debye-Scherrer equation [32]:

$$D = \frac{0.9\,\lambda_{k\alpha}}{B_{2\theta}\cos\theta} \tag{9}$$

where D is the particle size, 0.9 is the shape factors for spherical particles, λ is the radiation wavelength (1.5406 Å), $B_{2\theta}$ is the full width at half maximum, and θ is the angle at maximum intensity of the Al_2O_3 (110) and Ag (111). The value for the particle size of Al_2O_3 was 733.87 nm, while the Ag has a particle size of 24.9 nm.

3.5. Microstructure

3.5.1. Optical microscopy (OM)

In the micrographs of **Figure 7** that were obtained with the help of an optical microscope, they are observed the samples with silver inclusions in their different percentages 0.5, 1.0, 2.0, and 3.0% in

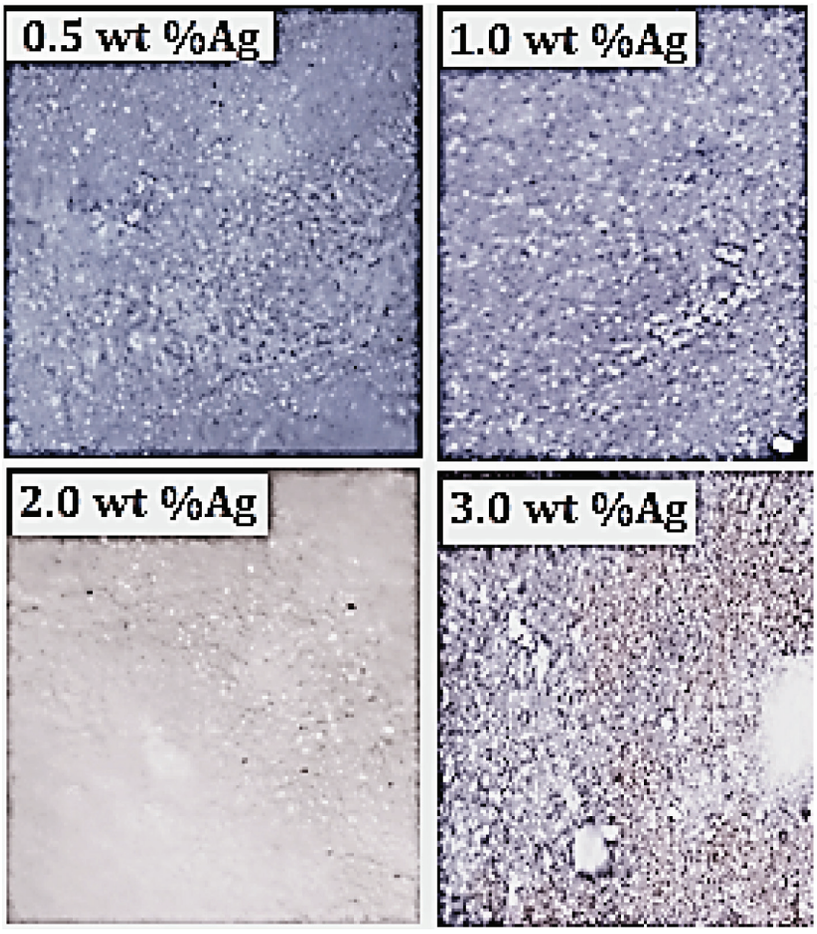

Figure 7. Micrographs of the samples sintered at 1500°C, during 2 h.

weight; these samples were sintered at 1500°C during 2 h. In the 0.5–1.0 wt% samples, they have visualized very fine microstructures with small grain size and evenly distributed. For the samples with 2.0–3.0 wt% silver a minimum grain growth is observed with respect to the previously mentioned samples, the grain size is observed small and uniform in most of the sample. This uniformity and control in grain growth are since the alumina was sintered in the presence of a liquid phase (molten silver), which allowed a filtration throughout the sample and the energy generated during the sintering was absorbed more evenly and due to this control in the grain growth.

3.5.2. Scanning electron microscopy (SEM)

Figure 8 shows the micrographs taken with the scanning electron microscope of the samples with inclusions of 0.0, 0.5, 1.0, 2.0 and 3.0% weight silver sintered at 1500°C during 2 h. In this figure it is possible to observe in all samples the presence of a very homogeneous microstructure with the presence of the matrix with a very fine second phase, the latter is well distributed in the matrix. No porosity is observed in any sample. This confirms previous density results, in where densities close to 100% of the relative density were reached. So the presence of the silver helps significantly consolidation of composites, and at the same time inhibits grain growth of the matrix. The microstructure with the characteristics obtained in these samples, combined with the grade of densification reached, suggests that composites with suitable mechanical properties will be obtained.

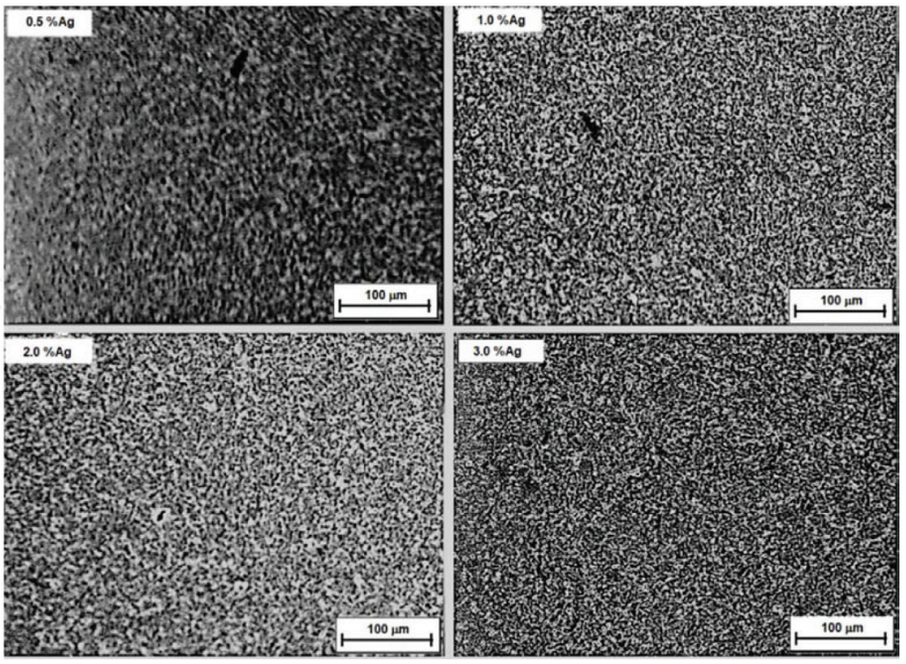

Figure 8. Micrographs of samples with different silver contents, sintered at 1500°C during 2 h.

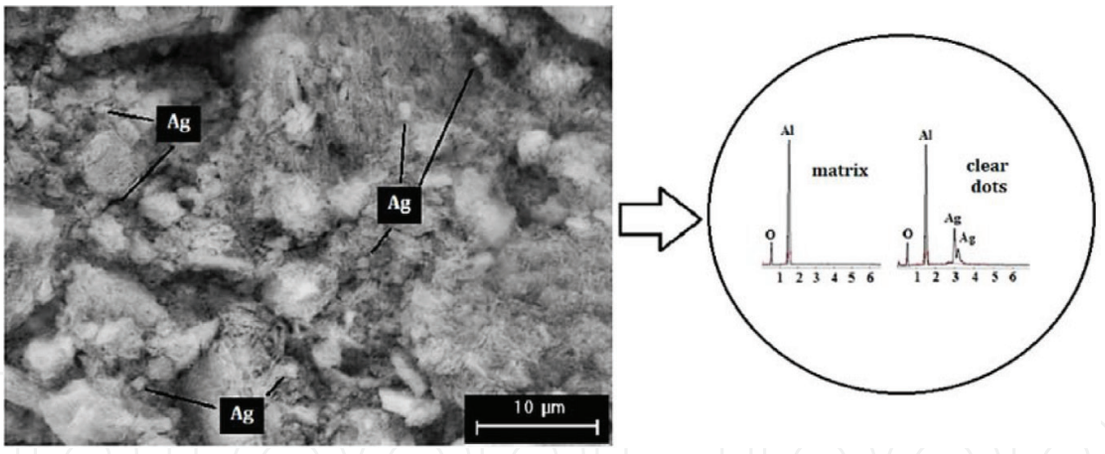

Figure 9. EDX microanalysis of sample with 2 wt% Ag sintered at 1500°C during 2 h.

3.5.3. Analysis by energy dispersive of X-rays (EDX)

Figure 9 presents the results of the analysis made by energy dispersive of X-rays performed in a punctual manner in the two phases (light and dark) that are observed in the microstructure of the samples with the different inclusions of silver. In spectra, the chemical elements present in each phase can be identified, the dark phase belongs to the matrix, and the elements found in this phase were oxygen and aluminum, indicating that this phase corresponds to alumina. The bright phase belongs to the inclusion present in the matrix, here the elements aluminum, oxygen, and silver were found, which means that the 2nd phase present in the microstructure is the silver added to the ceramic matrix as the reinforcement material.

3.6. Mechanical properties

3.6.1. Elastic modulus

Figure 10 shows the result of the measurements of the elastic modulus of the samples with different inclusions of silver. The value reported with its respective standard deviation is the average of 20 measurements made for each sample. The graph shows a decrease in the modulus of elasticity as the number of silver particles increases specifically for 1.0, 2.0, and 3.0 wt% silver with respect to the average value of the monolithic alumina. These results present a tendency similar to that shown in the density results of sintered samples; this means that samples with higher densification have less porosity. Consequently, they present more rigid bodies, the reason why a greater load is required to deform them. The elastic modulus is a measure of the stiffness of materials, in such a way that more rigid and fragile bodies have a higher value of elastic's modulus, that is why the high value of elastic's module in the sample of 0.5 wt% silver, does not have enough material to be less rigid. On the other hand, a ductile material such as metals in this case silver has lower elastic's modulus than alumina. Concerning the sample without inclusions of silver 0.0 wt%, a result is observed slightly below the monolithic alumina and slightly higher than the samples with 1.0, 2.0, and 3.0 wt% silver.

3.6.2. Flexural strength

In the same **Figure 10**, it can be observed the results obtained of flexural strength made to the samples with inclusions of 0.0, 0.5, 1.0, 2.0, and 3.0 wt% silver. The reported result is the average of 10 measurements made to each of the samples; the three-point bending test was used to obtain these results. The graph of **Figure 10** shows a similar behavior to that obtained in the density of the sintered samples as in the elastic's modulus, because the sample with 0.5 wt% silver reached the highest value, in this case, flexural strength, and above the average value of monolithic alumina. It is also observed that when silver increases in the composite there is

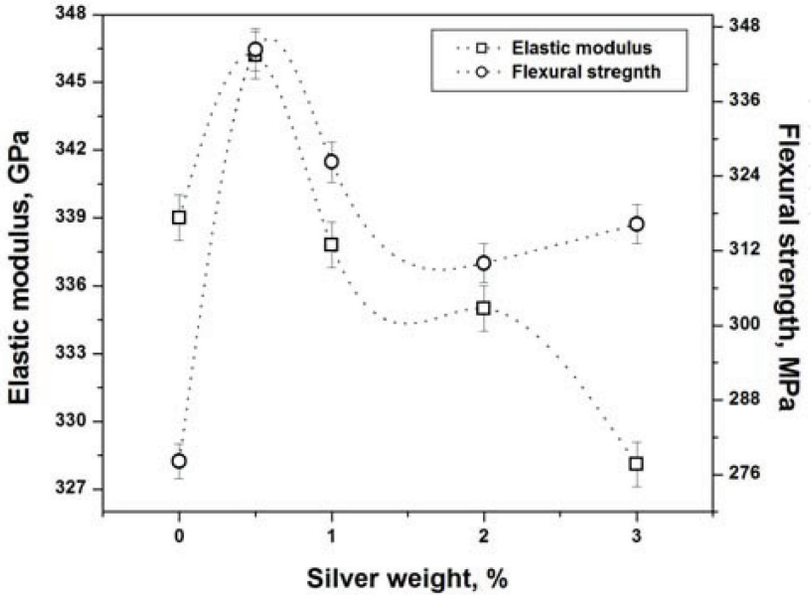

Figure 10. Elastic's modulus and flexural strength of the samples sintered at 1500°C during 2 h.

a downward trend. With respect to the sample with 0.0 wt% silver, a well below value was obtained in comparison with the samples with silver inclusions, as well as the value of monolithic alumina reported in the literature. With these results, it is determined that the inclusion of silver does not affect the flexural strength due to the good distribution of the particles during milling and to the sintering which helped to avoid the formation of defects in the sample.

3.6.3. Microhardness

Figure 11 reports the average and its standard deviation result of 20 measurements of the microhardness made in the samples sintered at a temperature of 1500°C during 2 h with different inclusions of silver. In **Figure 11** it is possible to observe that in the samples with higher silver inclusions the hardness values tend to increase slightly as the amount of silver increases. In these results, the positive effect of the silver particles is observed. With respect to the sample with 0.0 wt% silver, it was obtained a much lower value of microhardness than that obtained in the samples reinforced with silver, as well as that of the monolithic alumina reported in the literature. This result is due to the uncontrolled growth of the grains during sintering.

3.6.4. Fracture toughness

In the same **Figure 11** are shown the fracture toughness results obtained by the indentation fracture method in the sintered samples at a temperature of 1500°C during 2 h. The fracture toughness results reported are the average of 20 tests performed on each sample.

One of the most important observations in this figure is that in the samples with silver inclusions, values obtained are well above the average of the monolithic alumina. This improvement in fracture toughness is more significant in samples with 2.0–3.0 wt% silver. In the late sample, the improvement of fracture toughness reaches 450% more than the value of monolithic alumina. In agreement with the density results and the microstructure presented by the samples, these enhances in fracture toughness is due to the having a sample with very small grain sizes and

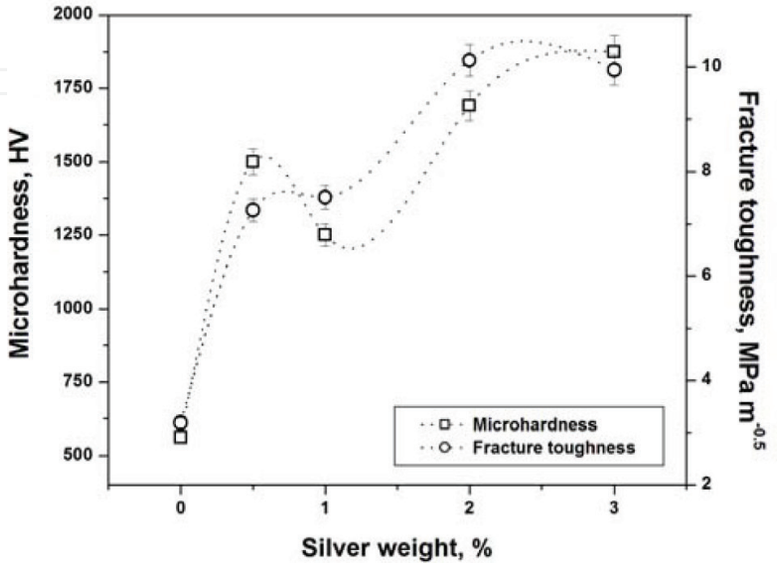

Figure 11. Microhardness and fracture toughness of the samples sintered at 1500°C for 2 h.

with a homogeneous distribution of the reinforcements in the matrix. For this reason, when in the ceramic matrix a cracking is generated, and it tries to propagate, there is a high possibility that the crack will meet or collide with some of the silver particles which act as metal bridges. This effect causes the crack to stop due to the ductility of the metal, or try to dodge it. Hence, the high values of tenacity obtained. With respect to the sample without silver inclusions, a result is observed that is much lower than that obtained in the samples reinforced with silver, as well as the average of the monolithic alumina due mainly to the disordered growth of the grains during sintering, as well as to the absence of a metallic agent or bridge that contributes to avoiding the propagation of cracks.

3.6.5. Indentation prints and fracture mechanism

Some authors have determined that the improvements in the properties of ceramics reinforced with metallic particles are due to the mechanical properties of the metal [5]. Then it can be said that ductility of silver is a factor that influences the improvement of the tenacity in the alumina. The silver particles which are distributed in a homogeneous way as shown in **Figures 7** and **8**, with their plastic deformation form bridges of fissures that absorb the energy of a crack when it is generated. These bridges cause the crack to stop or seek to avoid the metallic bridge, in such a way that it requires more energy to keep growing, slowing down and even being able to stop the advance of the same. **Figure 12** shows a crack in the sample reinforced with 0.5 wt% silver, that when it encounters a particle of ductile silver, it stops or diverts its trajectory, requiring more energy to continue advancing. In this way, it is proved that the mechanism of reinforcement of alumina by silver is due to the deflection of cracks. With this, we can comment that the overall silver objective which was at the beginning of this work was reached: Obtaining alumina-based ceramic materials (Al_2O_3) reinforced with Ag nanoparticles with high fracture toughness, through powder techniques.

A second study was performed only for samples with silver inclusions of 0.0 and 0.5 wt% under the same grinding settings. However, there were considered other sintering conditions such as time of 2 h varying the sintering temperature at 1400, 1500, and 1600°C. Besides, a sintering temperature of 1500°C varying the sintering time to 1, 2, and 3 h, heating speed of 5°Cmin^{-1}, as

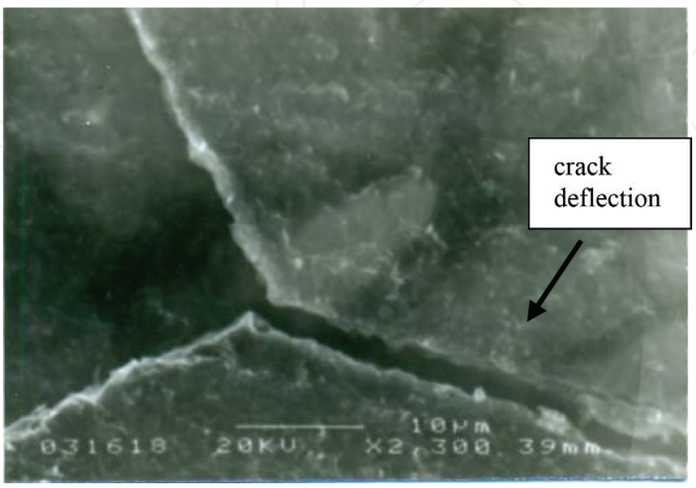

Figure 12. Crack deflection by a silver particle present in the sample with 2.0 wt% Ag.

well as the argon gas flow of 10 cm^3min^{-1}. It should be noted that these samples were selected because they presented the highest fracture toughness values. For the characterization of the samples, only the relative density tests of sintered samples, contraction of the samples, analysis of the microstructure by MO, microhardness, and fracture toughness were considered.

3.7. Density

Figure 13 shows the results of the relative density of the samples of both pure alumina and alumina reinforced with 0.5 wt% silver, which was sintered at a temperature of 1500°C during 1, 2 and 3 h. In the monolithic alumina samples, it is observed in the densification an increase with linear tendency with increments of sintering time. While, in the samples of 0.5 wt% silver it is observed a minimum increase in the densification when increasing the time from 1 to 2 h, but a considerable increase is reached at 3 h sintering time. Hence, an effect can be determined by improving results in silver when the samples are densified during 3 h at 1500°C. In the same **Figure 13** are observed the results of the relative density of the samples with inclusions of 0.0–0.5 wt% silver sintered during 2 h at 1400, 1500, and 1600°C. In pure alumina samples, an increase in densification is observed when the sintering temperature is increased, obtaining a greater densification when samples were sintered at 1600°C. Whereas, in the samples reinforced with 0.5 wt% silver, a considerable increase in the densification is observed in the sintered samples at 1600°C compared with the sintered samples at 1400–1500°C. Therefore, it can be determined that the temperature of 1600°C is the ideal for obtaining a greater densification in the composites.

3.8. Contraction

Figure 14 shows the results of the contraction of the samples with 0.0 and 0.5 wt% silver, which were sintered at 1500°C during 1, 2, and 3 h. It can be seen that the contraction in the

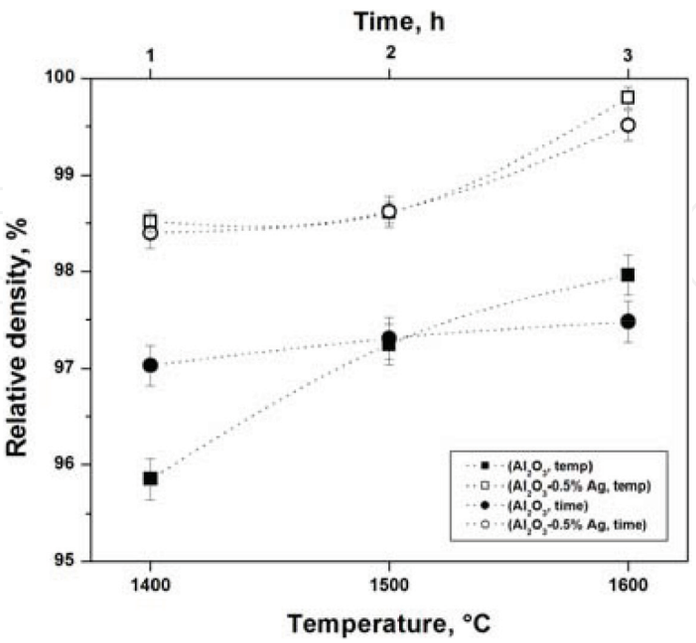

Figure 13. Relative density of the samples as a function of time and sintering temperature.

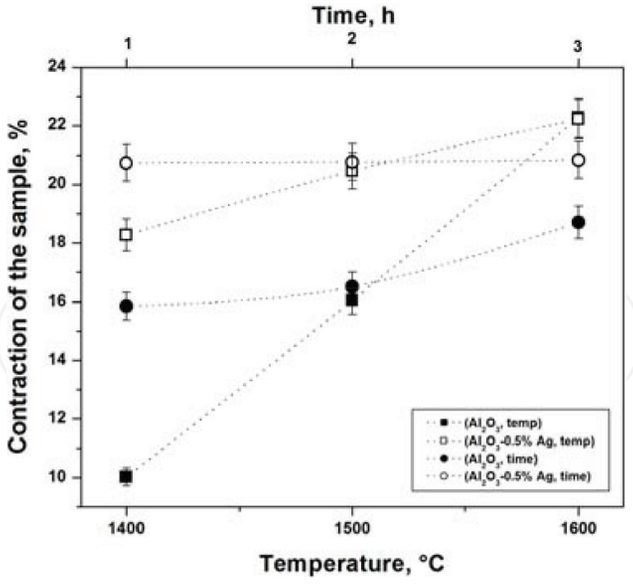

Figure 14. Contraction of the samples as a function of time and sintering temperature.

samples with silver does not present a significant variation. While, in samples of alumina without silver a different trend can be observed, and with an increasing tendency as the sintering time increases. However, it is significant the greater contraction in the samples with silver compared to the samples without silver. This behavior is due to the good thermal conductivity of the silver that favors the sintering phenomena. In the same **Figure 14** the results of the contraction of the samples are observed, when they were sintered during 2 h at 1400, 1500, and 1600°C. It can be observed that in the samples without silver, the contraction is more significant every time the sintering temperature tends to increase. In samples with silver inclusions, it is observed an increase in less drastic shrinkage. From the interpretation of the results it can be determined that the silver inclusions allow obtaining samples with a greater contraction during the sintering stage, and therefore, obtain more densified samples.

3.9. Microstructure by optical microscopy (OM)

Figure 15a shows the micrographs obtained from the optical microscope of the samples reinforced with 0.5 wt% silver sintered during 2 h at 1400, 1500, and 1600°C. They display very fine microstructures with small grain size and uniformly distributed. Minimal grain growth is observed although the temperature has varied. This uniformity and control in grain growth are because that most of the silver particles were sintered in the presence of a liquid phase, which allowed a filtration throughout the sample and the energy generated during the sintering was absorbed more uniformly, and due to this, there is the control on grain growth. In the **Figure 15b** the micrographs of the samples with 0.0 wt% silver sintered for 2 h are observed varying the temperature 1400, 1500, and 1600°C. In the images, it can see a microstructure very different from the one obtained in the samples with 0.5 wt% silver, in these figures it is difficult to determine and appreciate the distribution of the sizes of the grains. However, the importance of the addition of metallic particles in the matrix can be mentioned and emphasized to control the growth, distribution of the grains and consequently improvement in the mechanical properties.

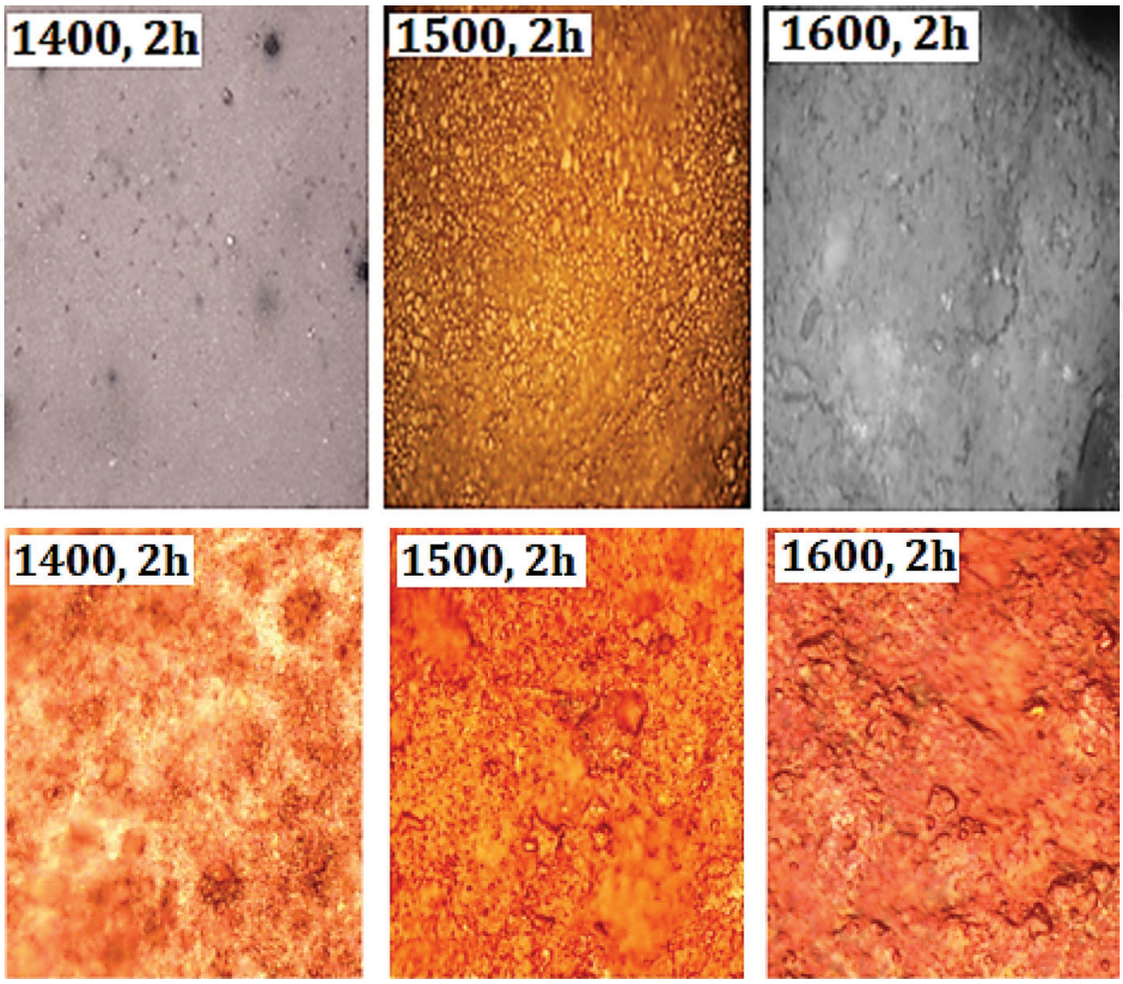

Figure 15. (a) Samples with 0.5 wt% Ag varying the sintering temperature. (b) Samples with 0.0 wt% Ag varying the sintering temperature.

3.10. Microhardness

Figure 16 shows the microhardness results of the samples with inclusions of 0.0 and 0.5 wt% silver sintered at a temperature of 1500°C with time variation of 1, 2, and 3 h. For the sample with 0.5 wt% Ag it can be seen in the graph that the sample sintered for 1 h obtained values below the monolithic alumina.

For the sample sintered during 2 and 3 h, it can be observed that with the inclusion of silver the value is very similar to that of the monolithic alumina. In this **Figure 16** also are observed the values of the samples of alumina with 0.0 wt% silver sintered with somewhat similar conditions. For the samples sintered for 1 and 2 h, a very similar value was obtained while, for a sample sintered for 3 h, the result was improved. However, it is well below the average of monolithic alumina. In the same **Figure 16** are observed the results of the samples with inclusions of 0.0 and 0.5 wt% silver sintered at different temperatures 1400, 1500, and 1600°C. For the sample with 0.5 wt% Ag it is observed in this figure that the sample sintered at 1400°C obtained a value well below the average of the monolithic alumina for the samples sintered at 1500 and 1600°C the results increased significantly. In the case of the

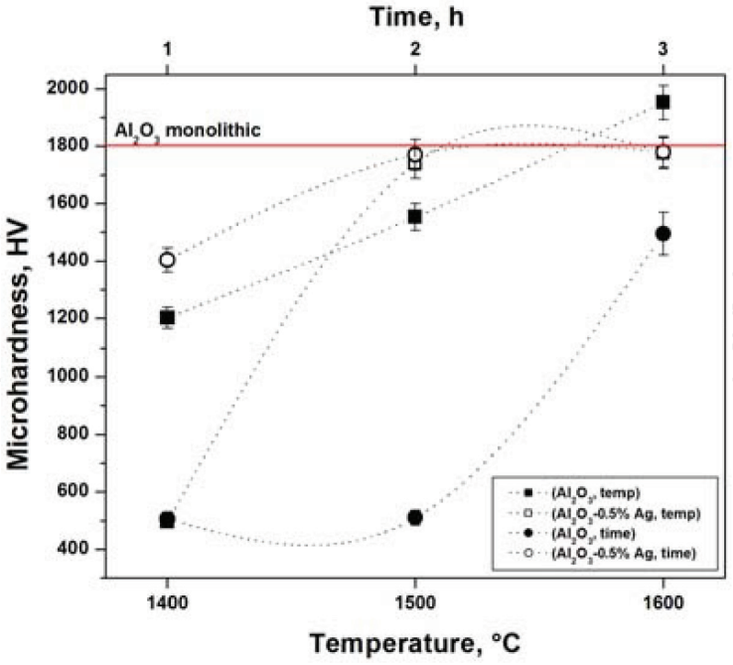

Figure 16. Microhardness of the samples as a function of time and sintering temperature.

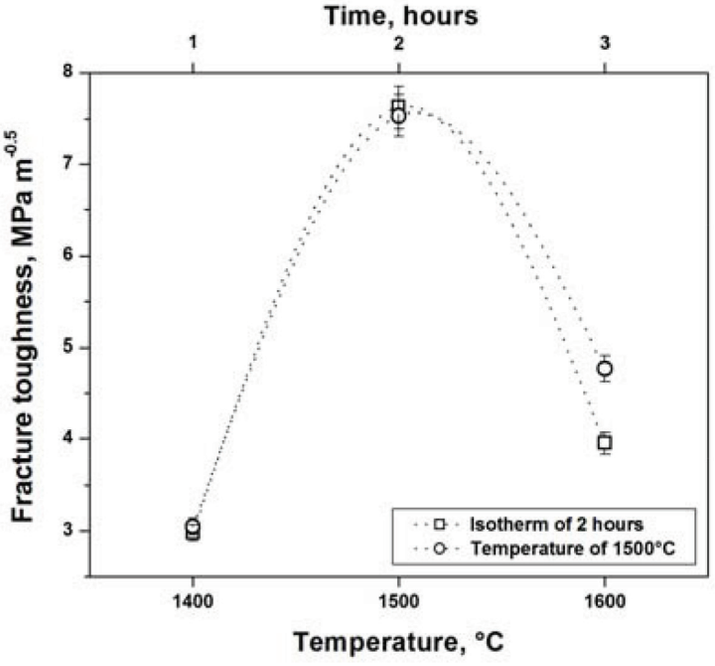

Figure 17. Fracture toughness results as a function of both sintering time and sintering temperature.

sintered sample at 1600°C it obtained a value very similar to that of the monolithic alumina, and in the case of the sample sintered 1500°C the value reached in the previous results was reduced a little. Regarding the samples without silver inclusions, a considerable increase is observed as the sintering temperature is increased. The hardness values of the samples sintered at 1400 and 1500°C were well below the average value of the monolithic alumina, but the sample sintered at 1600°C obtained a value slightly above the average value.

3.11. Fracture toughness

The results of the fracture toughness of the sintered samples varying the temperature and time are presented in **Figure 17**, in which a very similar behavior of the results can be observed. The samples with 0.5 wt% silver at 2 h at a temperature of 1500°C have values above the average of the monolithic alumina, showing a tendency opposite to previous results since as it increases the temperature and the time the value tends to decrease. In both cases, results are presented with an increasing tendency, and the importance of the sintering temperature in obtaining less fragile ceramics is demonstrated.

4. Conclusions

- Through the processing methodology proposed, dense alumina-based composites toughened with Ag nanoparticles were obtained.
- Grinding conditions used in this work were effective, as they managed to obtain particles with nanometric sizes.
- The fracture toughness of the Al_2O_3 was improved up to 450% with the reinforcement of the same by means of Ag nanoparticles homogeneously distributed in the ceramic matrix.
- Probably toughening mechanism of Al_2O_3 is owing to metallic bridges formed by the presence of ductile silver particles in the ceramic matrix.

Acknowledgements

The laboratories facility and the economic support given by UPV are appreciated. In addition, ERR is grateful to CONACyT for the funding given to carry out this work through Project 270294.

Conflict of interest

Compliance with ethics guidelines the authors declare that they have no conflict of interest or financial conflicts to disclose.

Author details

Enrique Rocha-Rangel*, Azucena Pérez-de la Fuente, José A. Rodríguez-García,
Eddie N. Armendáriz-Mireles and Carlos A. Calles-Arriaga

*Address all correspondence to: erochar@upv.edu.mx

Victoria Polytechnic University, Ciudad Victoria, Tamaulipas, México

References

[1] Serope K, Steven R. Manufactura, Ingeniería y Tecnología. México: Pearson Educación; 2002. 1p

[2] Bawa HS. Procesos de Manufactura. México: Editorial Mc Graw Hill; 2007. 1p

[3] Leyva AG. Síntesis y caracterizacion de nano-estructuras de óxidos de metales de transición, Tesis doctoral. República Argentina: Universidad Nacional de General San Martín; 2007

[4] Singh DK. Fundamentals of Manufacturing Engineering. Florida: CRS Press; 2008. 1p

[5] Bansal NP, Boccaccini AR. Ceramics and Composites Processing Methods. New Jesey: John Wiley and Sons; 2012. 1p

[6] Wei WCJ, Wang SC, Cheng FH. Characterization of Al_2O_3 composites with fine Mo particulates, I. Microstructural development. Nanostructured Materials. 1998;**10**:965-981

[7] Freitag D. Progress and opportunities in the development and application of advanced ceramics. In: 14th International Conference on Ultra-High Temperature Materials; 2000

[8] Szafran M, Konopka K, Bobryk E, Kurzydłowski KJ. Ceramic matrix composites with gradient concentration of metal particles. Journal of the European Ceramic Society. 2007;**27**:651-654

[9] Ighodaro OL, Okoli OI. Fracture toughness enhancement for alumina systems: A review. International Journal of Applied Ceramic Technology. 2008;**5**:313-323

[10] Singh JP, Bansal NP, Goto T, Lamon J, Choi SR, Mahmound MM, Link G, editors. Processing and Properties of Advanced Ceramics and Composites IV. Ceramic Transactions. Vol. 234. New Jersey: John Wiley and Sons; 2012. 1p

[11] Narayan R, Bose S, Bandyopadhyay A, editors. Biomaterials Science: Processing Properties and Applications II. Ceramic Transactions. Vol. 237. New Jersey: John Wiley and Sons; 2012. 1p

[12] Singh JP, Bansal NP, Ko SW, Castro RH, Pickrell G, Manjooran J, Nair KM, Singh G, editors. Processing and Properties of Advanced Ceramics and Composites V. Ceramic Transactions. Vol. 240. New Jersey: John Wiley and Sons; 2013. 1p

[13] Singh JP, Bansal NP, Bhalia AS, Mahmound MM, Manjooran N, Singh G, Lamon J, Choi SR, Pickrell G, Lu K, Brennecka G, Goto T, editors. Processing and Properties of Advanced Ceramics and Composites VI. Ceramic Transactions. Vol. 249. New Jersey: John Wiley and Sons; 2014. 1p

[14] Basu B, Balani K. Advanced Structural Ceramics. New Jersey: John Wiley and Sons; 2011. 1p

[15] Chung YW. Introduction to Materials Science and Engineering. Florida: CRC Press; 2006. 1p

[16] Daguano JKMF, Santos C, Souza RC, Balestra RM, Strecker K, Elias CN. Properties of ZrO_2-Al_2O_3 composite as a function of isothermal holding time. International Journal of Refractory Metals and Hard Materials. 2007;**25**:374-379

[17] Liu C, Zhang J, Sun J, Zhang X. Addition of Al-Ti-B master alloys to improve the performances of alumina matrix ceramic materials. Ceramics International. 2007;**33**:1319-1324

[18] Ko SJ, Min KH, Kim YD. A study on the fabrication of Al_2O_3/cu nanocomposite and its mechanical propertie. Journal of Ceramic Processing Research. 2002;**3**:192-194

[19] Rocha-Rangel E, Moreno-Guerrero MS, Velásquez-Naranjo A, Refugio-García E. Synthesis of Al_2O_3-Ni_3Al cermets by room-temperature ball milling of Al, Ni and Al_2O_3 mixtures. Materials Science Forum, "Advanced Structural Materials II". 2006;**509**:205-210

[20] Yao X, Huanga Z, Chena L, Jianga D, Tana S, Michel DI, Wang G, Mazerolles L, Pastol J. Alumina–nickel composites densified by spark plasma sintering. Materials Letters. 2005; **59**:2314-2318

[21] Sekino T, Nakajima T, Niihara K. Mechanical and magnetic properties of nickel dispersed alumina-based nanocomposite. Materials Letters. 1996;**29**:165-169

[22] Guichard JL, Tillement O, Mocellin A. Alumina-chromium cermets by hot-pressing of nanocomposite powders. Journal of the European Ceramic Society. 1998;**8**:1143-1152

[23] Ji Y, Yeomans JA. Processing and mechanical properties of Al_2O_3-5 vol.% Cr nanocomposites. Journal of the European Ceramic Society. 2002;**22**:1927-1936

[24] Prielipp H, Knechtel M, Claussen N, Streiffer S, Miillejans H, Ruhle M, Rodel J. Strength and fracture toughness of aluminum/alumina composites with interpenetrating networks. Materials Science and Engineering. 1995;**A197**:19-30

[25] Konopka K, Szafran M. Fabrication of Al_2O_3-Al composites by infiltration method and their characteristics. The Journal of Materials Processing Technology. 2006;**175**:266-270

[26] Shackelford JF, Alexander W. Materials Science and Engineering Handbook. Florida: CRS Press; 2001. 1p

[27] Vlack LM. Physical Ceramics for Engineering. Massachusetts: Addison Wesley Publishing Company; 1964. 1p

[28] Auerkari P. Mechanical and Physical Properties of Engineering Alumina Ceramics. Espoo: Technical Research Centre of Finland; 1996. pp. 3-36

[29] Rahaman MN. Ceramic Processing and Sintering. New York: Marcel Dekker Inc.; 2003. 1p

[30] Baudin C, Moya JS. Sinterización en estado sólido. Boletín de la Sociedad Española de Cerámica y Vidrio. 2007;**22**:133-142

[31] Evans AG, Charles EA. Fracture toughness determinations by indentation. The Journal of the American Ceramic Society. 1976;**59**:371-372

[32] Holzwarth U, Gibson N. The Scherrer equation versus the 'Debye-Scherrer equation. Nature Nanotechnology. 2011;**6**:534-539

IntechOpen